Analysis and Prediction of Vegetation Cover in Antioquia Using Sentinel-2 Satellite Images

Felipe Rodriguez Angel
Departamento de Ingeniería de Sistemas
Universidad de Antioquia
Medellín, Colombia
felipe.rodrigueza@udea.edu.co

Jagler David Velasquez Velasquez
Departamento de Ingeniería de Sistemas
Universidad de Antioquia
Medellín, Colombia
jagler.velasquez@udea.edu.co

Abstract* — *Changes in vegetal mass are relevant indicators of threats to biodiversity. The vast amount of current satellite images allows for the assessment and evaluation of multiple terrestrial environmental conditions. Nevertheless, the automation of change detection remains a challenge that constantly requires new algorithms and methods. Machine Learning methods are enabling the tackling of many of these challenges, although they require a large amount of labeled data. In this project, the monitoring of forest mass in Antioquia will be addressed through publicly available satellite images from the Sentinel-2 Earth observation mission.

Keywords*— *Colombia - Machine Learning - Sentinel-2 - Vegetation - Geospatial observation

I. INTRODUCTION

This work aims to expand the scope of environmental monitoring by applying Machine Learning techniques to Sentinel-2 satellite imagery for comprehensive vegetation monitoring in Antioquia. The significance of this study is underlined by alarming statistics: approximately 17.8% of Colombia's vegetation loss in 2017 occurred in Antioquia [19]. This alarming rate of vegetation loss highlights the urgent need for innovative monitoring methods.

The task is challenging due to the vastness of Antioquia, encompassing approximately 63,612 km² [20], and its diversity, housing 89 recognized ecosystems [21]. Each ecosystem presents unique characteristics when observed from satellite imagery, adding complexity to the monitoring process. To tackle these challenges, we developed a custom Deep Learning architecture named *"VGGUdeaSpectral"*. This model, inspired by the VGG architectures, incorporates a SpectralAttention mechanism to enhance feature detection, tailored to the varied ecosystems. The architecture's name pays homage to our institution, Universidad de Antioquia (UdeA), acknowledging its role in this innovative endeavor.

Further, we adopted a grid-based approach to divide the region of interest into contiguous tiles. This method transforms the dataset of our *region* into a manageable vector of contiguous rasters, enabling more efficient processing and analysis. This approach not only addresses the challenge of the region's size and diversity but also allows for detailed, localized vegetation monitoring.

By combining advanced Machine Learning techniques with a strategic grid-based approach, this project sets out to provide a novel solution to the critical challenge of vegetation monitoring in a region marked by both environmental diversity and ecological vulnerability.

II. SYSTEM VARIABLES AND TARGET VARIABLE

The following section provides a detailed explanation of the system variables and their method of acquisition.

A. INPUT VARIABLES

These consist of rasters obtained from the Sentinel-2 satellite. More details can be seen in Table I.

Input Variables		**Target Variables**	
Properties	**Values**	Tree Vegetation Coverage Percentage (PTC)	0 - 100%
Width(pixels)	100		
Height/(pixels)	100		
Bands	3		
File Type	.tif	Non-Tree Vegetation Coverage Percentage (PNV)	0 - 100%
Coverage per pixel	$10m^2$		
Area covered per each image	$1Km^2$		
Total of Images	64106		

Table I. Properties of SENTINEL--2's Input Variable

Figures 1 and 2 show four histograms: three for the R (red), G (green), and B (blue) bands of Sentinel-2 satellite images in Antioquia, and one for the "TargetData (y)", indicating the percentage of vegetation coverage. More details on this can be seen in Table II. In the fourth histogram, most frequencies are concentrated towards higher percentages, with a peak near 100%. This predominance suggests that there are more observations with high percentages of vegetation coverage and fewer with low percentages.

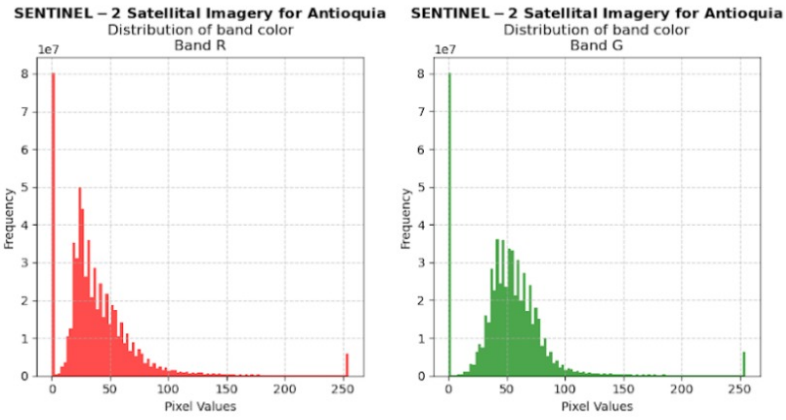

Figure 1. Pixel Distribution for Red and Green Color Channels

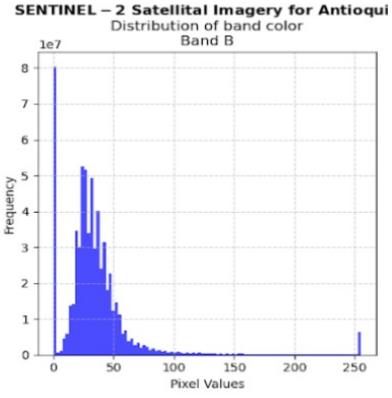

Figure 2. Pixel Distribution of Blue Color Channels

A.1. Data Balance of the Input Variables

The balance and distribution of input data are pivotal to the development of robust machine learning models. Sentinel-2 satellite imagery for Antioquia provides a rich dataset for analyzing vegetation cover. The histograms in Figures 1 and 2 illustrate the pixel value distributions for the respective color bands captured by the satellite.

Figure 1 showcases the pixel distribution for the Red (Channel R) and Green (Channel G) color channels. The Red channel histogram displays a steep peak in the lower pixel values, suggesting a high frequency of darker tones which are indicative of dense vegetative areas. Conversely, the Green channel histogram, while also demonstrating a skew towards lower pixel values, has a more gradual decline and spread across the value range, which can be attributed to the varying shades of vegetation present in the region.

Figure 2 presents the pixel distribution for the Blue (Channel B) color channel. The histogram reveals a concentration of lower pixel values with a noticeable peak, followed by a tail extending towards the higher values. This is consistent with the natural reflectance properties of vegetation in the blue band, where vegetation generally reflects less blue light compared to green.

The predominance of lower pixel values across all bands signifies a substantial presence of vegetative cover. The specific characteristics of these three bands can be seen explained on Table II.

Name	Units	Min	Max	Pixel Size	Wavelength / Classification	Description
B2		0.0001		10 meters	496.9mm (S2A) / 492.1mm (S2B)	Blue
B3		0.0001		10 meters	560mm (S2A) / 559mm (S2B)	Green
B4		0.0001		10 meters	664.5mm (S2A) / 665mm (S2B)	Red
MSK_CLDPR	0	0	100	20 meters	Does not relate magnetic wavelength	Cloud Probability Map

Table II. Description of Bands used from the SENTINEL-2 instrument

B. TARGET VARIABLE AND MODEL OUTPUT

The output of the model will be represented as a percentage value ranging from 0 to 100. The target variable during training is composed of a combination of the two bands from the MODIS instrument.

The goal is to predict vegetation cover, for which Equation I will be used. In this equation, the percentage values obtained from *Percent_Tree_Cover(PTC)* and *Percent_NonTree_Vegetation* (PNV) will be summed to obtain a new variable called Percent_Vegetation_Coverage (PVC). This variable represents the percentage, within an interval [0%, 100%], of an image that is covered by vegetation, both from trees and non-tree sources. The calculation is defined like this:

$$PVC = PTC + PNV \quad (I)$$

Integrity Considerations: Due to measurement errors from the instrument (usually caused by the presence of clouds, aerosols, or gradual inclinations of the tool), some pixels may sum to values greater than 100%. The values of this variable are truncated to ensure they never exceed 100% (there are no values less than 0, hence truncating the lower interval is not necessary).

B.1. Data Balance of the Target Variable

The distribution of the vegetation coverage percentage shows clear signs of imbalance. There is a noticeable increase at the right end of the histogram for the target variable, as can be seen in Figure 3 (high percentages of vegetation coverage) which prevail in the dataset. This imbalance can introduce biases into the machine learning model, making it more accurate in predicting areas with high vegetation coverage and less precise for areas with low coverage due to the scarcity of data in that range.

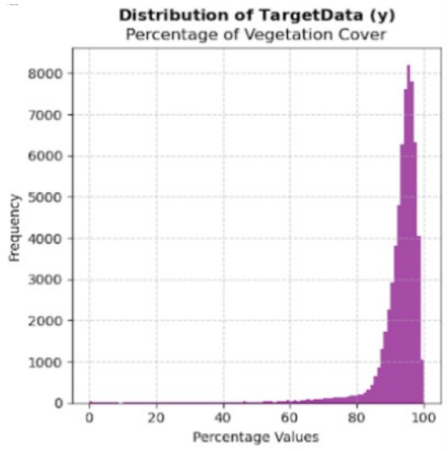

Figure 3. Distribution of Percentages of Vegetation Cover for the images in our Dataset

III. LITERATURE REVIEW

For this project, various articles addressing the same (or related) M.L problems were taken into account. The first, "Sentinel-2 and Sentinel-3 Intersensor Vegetation Estimation via Constrained Topic Modeling" [2], has an approach directly related to the modeling techniques of the course, specifically proposing an unsupervised approach to the vegetation target variable. The second article, "Development of Machine Learning Based Approach for Computing Optimal Vegetation Index with The Use of Sentinel-2 And Drone Data" [3], proposes a machine learning architecture for addressing the prediction problem. The third, "Critical Analysis of Machine Learning Approaches for Vegetation Fractional Cover Estimation Using Drone and Sentinel-2 Data" [4], compares different approaches to predicting fractional vegetation cover, which is equivalent to the problem being addressed and uses the same data being used in this problem (Sentinel-2 [2]). The fourth, "Forest Change Detection in Incomplete Satellite Images With Deep Neural Networks" [5], proposes an approach directly related to the course's modeling techniques, using deep neural networks; it details techniques to deal with cases where there are images with missing data, and the implemented model proved to be highly extrapolatable to regions other than those seen in training.

The results of the previous articles, the methodology used to validate the obtained results, as well as the learning techniques they implement, are related in Table III.

Artículo	Learning Technique	Validation Methodology	Results
Sentinel-2 and Sentinel-3 Intersensor Vegetation Estimation via Constrained Topic Modeling [2]	Probabilistic Constrained Latent Semantic Analysis (CpLSA) [6]	- Quantitative Evaluation of Mean Squared Error (MSE) [7] - Statistical Tests of Friedman and Holm [8]	**Normalized Difference Vegetation Index (NDVI) [7]:** -Sentinel-2: MSE avg= 0.0307 - Linear Regression: MSE avg = 0.0256 -SVR: MSE avg= 0.0314 - GPR: MSE avg= 0.0173 **Índice de Vegetación SAVI [7]:** - Sentinel-2: MSE promedio = 0.0357 -Linear Regression: MSE avg= 0.0278 -SVR: MSE avg= 0.0323 - GPR: MSE avg= 0.0213 - CpLSA: MSE avg= 0.0109
Development of Machine Learning Based Approach for Computing Optimal Vegetation Index with The Use of Sentinel-2 And Drone Data [3]	Neural Network based learning [9]	- Comparison of predicted results with ground truth[10] - Calculation of true positives [10]	- The proposal is capable of calibrating satellite-derived indices using machine learning [10] - The proposed methodology is capable of efficiently calibrating satellite-derived indices [10]
Critical analysis of machine learning approaches for vegetation fractional cover estimation using drone and sentinel-2 data [4]	-Support Vector Regression (SVR) [11] -Random Forest Regression (RFR) [11] -K-Nearest Neighbors (KNN) [11] -Linear Regression (LR) [11]	- R^2 (Coefficient of determination) [12] - Cross-validation (K-fold cross-validation) [12] - Root Mean Squared Error (RMSE) [12] - Mean Bias[12] - Average Relative Error (ARE) [12]	**Input features: NDVI+SAVI [13]** -RMSE: 0.159 -Mean Bias: -0.093 -ARE: 0.17 **Input features: SAVI+PAVI [13]** -RMSE: 0.163 -Mean Bias: -0.097 -ARE: 0.20 **Input features: NDVI+SAVI+PAVI [13]** -RMSE: 0.163 -Mean Bias: -0.091 -ARE: 0.19
Forest Change Detection in Incomplete Satellite Images with Deep Neural Networks [5]	Convolutional Neural Networks (CNN) [14]	10-fold cross validation [15]	-Average classification rate of last-generation patches of 91.6% [14] -Average prediction error of onset/offset of 4.9 months [14]

Table III. Comparative table of the related articles from the literature review

IV. EXPERIMENTS

Satellite images with atmospheric and earth surface information were obtained using the database from the MultiSpectral Instrument Sentinel-2 [2]. Additionally, MODIS/Terra Vegetation Continuous Fields Yearly L3 Global 250 m SIN Grid [16] was used to obtain satellite rasters related to forest cover. The dataset consists of 64,106 images, each of 100 x 100 pixels, representing 10m² per pixel and 1Km² in total, with three bands. Each image is the result of averaging photographs taken throughout the year in a specific region. Figure 3 shows the region of Antioquia to which these images correspond. For validation, K-fold Cross Validation was used, and hyperparameters were optimized using Grid Search and Random Search with the Sklearn library.

The Mean Absolute Error Loss Average (MAE Loss Avg) was used as the driving metric for the optimization process, and the Root Mean Square Error Loss Average (RMSE Loss Avg) was used to evaluate system performance, giving greater penalties to predictions that were far from the true values (y_true).

The main measure for the optimization process is the MAE Loss (avg), while RMSE was calculated as a complementary measure to be used when analyzing the results.

Three models were evaluated and implemented: Multiple Regression, Parzen Window implemented through a KmeansRegressor, and Convolutional Artificial Neural Network with an Spectral Attention mechanism

Figure 4. Overlapping of GEOJSON geometry (orange) with the raster images as tiles of 1km2

A. MULTIPLE REGRESSION MODEL

A set of hyperparameters was defined, with which the model performed combinations during training. These can be seen in Table IV, where the combination that yielded the best results is highlighted in bold.

Hyperparameters	Values
fit_intercept	[**True**, False]
copy_X	[**True**, False]
positive	[**True**, False]

Table IV. Hyperparameters used on the param_grid

GridSearchCV was used with the parameters from Table IV to find the combination of parameters that gave the best results, which can be seen in Table VII.

Using K-Folds, the data is split into two sets, one for training and one for validation. The model is trained with the training data and the time it takes is measured, then predictions are made with the validation set and using the predicted Y and the actual Y, the MAE Loss and RMSE Loss are calculated. Finally, a report is printed for the current fold and the process is repeated for the next fold.

B. VGGUdeaSpectral

A *CNN* called *VGGUdeaSpectral* is defined with *PyTorch compatibility*. An instance of *NeuralNetRegressor* is also created using the *skorch interface*. This allows us, through the compatibility *library Skorch*, to call *sklearn* utilities on our *PyTorch-based* model.

A hyperparameter search space called param_dist is defined, which contains different hyperparameter options. The combination that yielded the best results is shown in bold in Table VI.

Hyperparameters	Values
module__num_filters1	[32, 64, 128]
module__num_filters1	[64, 128, 256]
module__num_filters1	[128, 256, 512]
module__activation_type	['relu', 'sigmoid', **'tanh'**]
module__dropout_rate	uniform(0.2, 0.5) (**0.633088**)
module__fc1_out_features	[512, 1024, **2048**]
module__fc2_out_features	[256, **512**, 1024]
lr	[0.01, 0.001, **0.0001**]
max_epochs	[5, 10, **20**]

Tabla VI. Search space for our param_dist

The procedure for training the model and starting to use it to predict vegetation percentage is similar to the previous models, with the difference that in this case we must apply the Skorch compatibility layer to take advantage of the functionalities offered by *sklearn.RandomizedSearchCV*.

The results of the best parameter combination found by RandomizedSearchCV can be seen in Table VII.

Metric Results on the validation Metrics	Predictive Model		
	M.Regression	Parzen	VGG
MAE Loss Avg	4.659	10.211	3.7996
MAE Loss Std	0.0294	0.74575	---
RMSE Loss Avg	9.1526	17.5521	6.0441
RMSE Loss Std	0.1269	1.44146	---
Execution Time (seconds)	63.41	2867.55	28129.79

Table VII. Best results obtained on the validation process with the 3 models that were implemented

The code used to develop this project is available on GitHub [18]. It includes explanatory notebooks of the entire process, as well as scripts and instructions to run and train new models with the same workflow.

V. ANALYZING OUR RESULTS

The lowest Mean Absolute Error Loss Average (MAE Loss Avg) was achieved by the Artificial Neural Network (RNA) model, which was 3.79. This means that on average, the values predicted by the model differ from the actual values by 3.79 units. For example, if the predicted vegetation percentage is 70%, with an MAE Loss Avg of 3.79, the actual value would be between 66.21% and 73.79%. This implies that the smaller this value, the better the model's predictions. Based on the MAE Loss Avg, this is the best model out of the three.

On the other hand, the worst is the Parzen Window model, as its predictions differ by 10.21 units from the actual values. Using the previous example, if the predicted vegetation percentage is 70%, the actual value would be between 59.79% and 80.21%. If the goal is for the model to be as precise as possible, this model should not be considered.

The lowest Mean Absolute Error Loss Standard Deviation (MAE Loss Std) is that of the regression model, which was 0.0294 units. This value indicates the variance from one training to another, meaning the smaller it is, the more stable the model. In this case, the most stable model is the regression model.

In terms of time to train, the regression model was the fastest, taking approximately 1 minute. The longest was the RNA model, taking approximately 7.8 hours. The Parzen model took about 47 minutes.

VI. VALIDATING OUR RESULTS

To further test the capacity of our model to generalize and predict successfully (outside of the already applied cross-validation process), we decided to test on a different never seen by any of the models on any of the cross-validation steps. The original training was done with 2020 data, however, due to API access issues we were unable to access MODIS TERRA data from posterior years. Thus, we decided to apply this extra test with 2019 data. We are aware that methodologically is not adequate to test with previous years, but we find nonetheless this experiment valuable to better guide future work.
The results were as follows:

Model	MAE LOSS 2020	MAE LOSS 2019	RMSE LOSS 2020	RMSE LOSS 2019	MAE LOSS CHANGE (%)	RMSE LOSS CHANGE (%)
Multiple Regressor	4.659	4.612	9.1532	9.3915	+1.00% Improved	-2.60% Worsened
VGG Udea Spectral	3.799	4.437	6.0442	7.6646	-16.79% Worsened	-26.81% Worsened

Table VIII. Variance in best performing models with 2020 (train and validation data) to 2019 (test data)

Finally, a visualization of the results through the usage of two scatter plots (one for 2019, the other for 2020) allows us to better understand any bias on the predictions. The Figures 5 below provide valuable context.

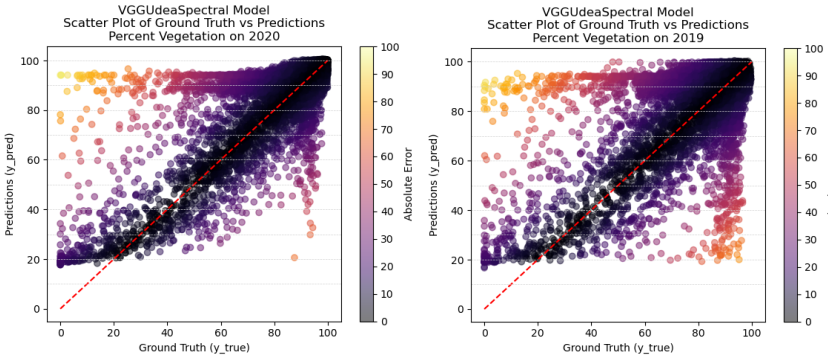

Figure 5. Scatter plot with VGGUdeaSpectral for years 2020 and 2019

On Figure 5, we can observe that the data points follow a similar distribution, although the points in 2019 are far less centered on the diagonal compared to our 2020 results. Also, a high number of the points is centered towards the 100% values, while most of the predictions with the highest absolute error are around the 0-40% vegetation coverage. These results confirm our hypothesis that the high imbalance of the training data worsened the results on the lower vegetation coverage zones, but nonetheless also show that our *VGGUdeaSpectral* model is capable of capturing part of the relationship between the satellital images and the output variable.

Figure 6 shows us that our *MultipleRegressor* was actually regressing over the median, and that the deceitful

performance shown by the *RMSE* and *MAE* metrics was made possible by the imbalance in the data. This shows us that the *Multiple Regressor*, being a simple model, was not able to find any meaningful patterns on the data, and serves as a cautionary tale to always validate the predictions without completely relying on metrics.

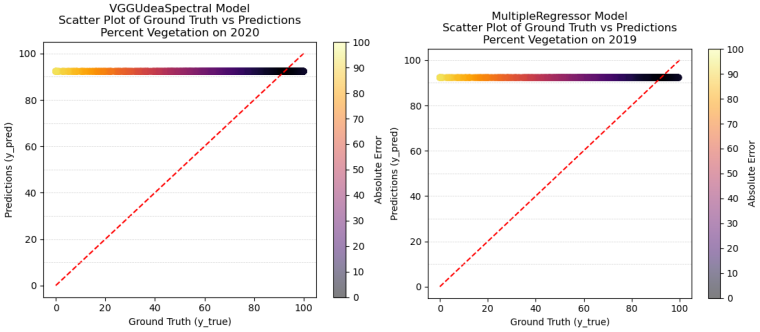

Figure 6. Scatter plot with MultipleRegressor for years 2020 and 2019

VII. SUMMARY

The MultipleRegressor is not a suitable model for this task due to its simplicity. Before any on-field deployment, the performance and reliability of the *VGGUdeaModel* will benefit greatly from an expanded hyperparameter optimization and training from an expanded time frame that adds broader generalization capabilities to the model which allows it to learn more complex atmospheric and ecological relationships that may not be present on the year on which it was trained. Lastly, the dataset imbalance problem may be addressed through the use of data augmentation techniques to increase the data points over the 40th percentile of vegetation coverage.

VIII. ACKNOWLEDGMENTS

We would like to thank our coordinator Dr. Raul Ramos Pollan for its invaluable feedback and support; we also would like to thank Carlos Andres Sanchez Aviles and Yeison Alexander Cordoba Mena for their help on the stylization and redaction of this work.

IX. REFERENCES

[1] “Geoportal DANE- Página de descarga”. DANE - Inicio. Accedido el 17 de octubre de 2023. [En línea]. Disponible: https://www.dane.gov.co/files/geoportal-provisional/index.html

[2] “Sentinel-2 MSI: MultiSpectral Instrument, Level-2A | Earth Engine Data Catalog | Google for Developers”. Google for Developers. Accedido el 17 de octubre de 2023. [En línea]. Disponible: https://developers.google.com/earth-engine/datasets/catalog/COPERNICUS_S2_SR

[3] A. Agarwal, S. Kumar and D. Singh, "Development of Machine Learning Based Approach for Computing Optimal Vegetation Index with The Use of Sentinel-2 And Drone Data," IGARSS 2019 - 2019 IEEE International Geoscience and Remote Sensing Symposium, Yokohama, Japan, 2019, pp. 5832-5835, doi: 10.1109/IGARSS.2019.8897896.

[4] A. K. Maurya, M. Nadeem, D. Singh, K. P. Singh and N. S. Rajput, "Critical Analysis of Machine Learning Approaches for Vegetation Fractional Cover Estimation Using Drone and Sentinel-2 Data," 2021 IEEE International Geoscience and Remote Sensing Symposium IGARSS, Brussels, Belgium, 2021, pp. 343-346, doi: 10.1109/IGARSS47720.2021.9554422.

[5] S. H. Khan, X. He, F. Porikli and M. Bennamoun, "Forest Change Detection in Incomplete Satellite Images With Deep Neural Networks," in IEEE Transactions on Geoscience and Remote Sensing, vol. 55, no. 9, pp.5407-5423, Sept. 2017, doi: 10.1109/TGRS.2017.2707528.

[6] R. Fernandez-Beltran, F. Pla and A. Plaza, "Sentinel-2 and Sentinel-3 Intersensor Vegetation Estimation via Constrained Topic Modeling," in IEEE Geoscience and Remote Sensing Letters, vol. 16, no. 10, pp. 1531, Oct. 2019, doi: 10.1109/LGRS.2019.2903231.

[7] R. Fernandez-Beltran, F. Pla and A. Plaza, "Sentinel-2 and Sentinel-3 Intersensor Vegetation Estimation via Constrained Topic Modeling," in IEEE Geoscience and Remote Sensing Letters, vol. 16, no. 10, pp. 1533, Oct. 2019, doi: 10.1109/LGRS.2019.2903231.

[8] R. Fernandez-Beltran, F. Pla and A. Plaza, "Sentinel-2 and Sentinel-3 Intersensor Vegetation Estimation via Constrained Topic Modeling," in IEEE Geoscience and Remote Sensing Letters, vol. 16, no. 10, pp. 1534, Oct. 2019, doi: 10.1109/LGRS.2019.2903231.

[9] A. Agarwal, S. Kumar and D. Singh, "Development of Machine Learning Based Approach for Computing Optimal Vegetation Index with The Use of Sentinel-2 And Drone Data," IGARSS 2019 - 2019 IEEE International Geoscience and Remote Sensing Symposium, Yokohama, Japan, 2019, pp. 5832, doi: 10.1109/IGARSS.2019.8897896

[10] A. Agarwal, S. Kumar and D. Singh, "Development of Machine Learning Based Approach for Computing Optimal Vegetation Index with The Use of Sentinel-2 And Drone Data," IGARSS 2019 - 2019 IEEE International Geoscience and Remote Sensing Symposium, Yokohama, Japan, 2019, pp. 5835, doi: 10.1109/IGARSS.2019.8897896

[11] A. K. Maurya, M. Nadeem, D. Singh, K. P. Singh and N. S. Rajput, "Critical Analysis of Machine Learning
Approaches for Vegetation Fractional Cover Estimation Using Drone and Sentinel-2 Data," 2021 IEEE International Geoscience and Remote Sensing Symposium IGARSS, Brussels, Belgium, 2021, pp. 343, doi: 10.1109/IGARSS47720.2021.9554422

[12] A. K. Maurya, M. Nadeem, D. Singh, K. P. Singh and N. S. Rajput, "Critical Analysis of Machine Learning
Approaches for Vegetation Fractional Cover Estimation Using Drone and Sentinel-2 Data," 2021 IEEE International Geoscience and Remote Sensing Symposium IGARSS, Brussels, Belgium, 2021, pp. 345, doi: 10.1109/IGARSS47720.2021.9554422

[13] A. K. Maurya, M. Nadeem, D. Singh, K. P. Singh and N. S. Rajput, "Critical Analysis of Machine Learning
Approaches for Vegetation Fractional Cover Estimation Using Drone and Sentinel-2 Data," 2021 IEEE International Geoscience and Remote Sensing Symposium IGARSS, Brussels, Belgium, 2021, pp. 346, doi: 10.1109/IGARSS47720.2021.9554422

[14] S. H. Khan, X. He, F. Porikli and M. Bennamoun, "Forest Change Detection in Incomplete Satellite Images With Deep Neural Networks," in IEEE Transactions on Geoscience and Remote Sensing, vol. 55, no. 9, pp. 5407, Sept. 2017, doi: 10.1109/TGRS.2017.2707528

[15] S. H. Khan, X. He, F. Porikli and M. Bennamoun, "Forest Change Detection in Incomplete Satellite Images With Deep Neural Networks," in IEEE Transactions on Geoscience and Remote Sensing, vol. 55, no. 9, pp. 5416, Sept. 2017, doi: 10.1109/TGRS.2017.2707528

[16] European Space Agency (ESA), "Sentinel-2 MultiSpectral Instrument (MSI) Level-2A," publicado por Google Earth Engine Organization, 2023. [Online]. Disponible:https://developers.google.com/earth-engine/datasets/catalog/COPERNICUS_S2_SR_HARMONIZED. [Accedido: 01-Oct-2023].

[17] LP DAAC, "MODIS/Terra Vegetation Continuous Fields Yearly L3 Global 250 m SIN Grid. Version 061," publicado por Google Earth Engine Organization. [Online]. Disponible: https://doi.org/10.5067/MODIS/MOD44B.061. [Accedido: 01-Oct-2023]

[18]Rodriguez,F. Udeai_forest.https://github.com/Felipe-RA/udeai_forest.

[19] Instituto de Hidrología, Meteorología y Estudios Ambientales (IDEAM), "IDEAM PRESENTA LOS DATOS ACTUALIZADOS DEL MONITOREO A LA DEFORESTACIÓN." [Online]. Available: https://shorturl.at/dBO39.

[20] "Geografía de Antioquia," Gobernación del departamento, Archivado desde el original el 5 de julio de 2015. [Online]. Available: https://web.archive.org/web/20150705154640/http://www.antioquia.gov.co/index.php/antioquia/datos-de-antioquia/9790.